

Characterization of Hybrid Carbon Fiber Composites using Photoluminescence Spectroscopy

Alex Selimov*, Ryan Hoover*, Quentin Fouliard*, and Albert Manero II*

University of Central Florida, Orlando, 32828, United States

Peter Dackus†, Declan Carolan‡, and Ambrose Taylor§

Imperial College London, London, UK

Seetha Raghavan¶

University of Central Florida, Orlando, 32828, United States

Hybrid carbon fiber reinforced polymers (HCFRPs) are a new breed of material that are currently being explored and characterized for next generation aerospace applications. Through the introduction of secondary reinforcements, such as alumina nanoparticles, it is possible to achieve improved mechanical behavior and enable structural sensing to create unique hybrid properties. The photoluminescent properties of the alumina inclusions allow for the application of local stress measurements through piezospectroscopy (PS) in addition to dispersion characterization. Measuring the shift in emission wavenumber at several points across the face of a sample allows for determination of the local stress through the application of the PS relationship. Measuring local intensity differences across the face of the sample, alternatively, allows for the determination of relative local particle concentration for dispersion characterization. Through investigation of an HCFRP sample loaded with 10 wt% of alumina nanoparticles, it was found that stress was greater in regions with high relative particle concentrations upon mechanical loading. Further investigation also found evidence of particle-matrix debonding, characterized by a lower particle stress response to increasing composite strain at higher loads. In order to address both of these issues silane coupling agents are utilized to adjust particle behavior. It is found that the use of these treatments results in improved particle dispersion and reduced sedimentation. A reactive and non-reactive surface treatment were compared and it was found that the reactive treatment was more effective at improving dispersion for the weight percentage investigated. The outcomes of this work demonstrate the potential of utilizing the photoluminescent sensing capability of these reinforcing particulates to tailor the design of the hybrid carbon fiber composites.

I. Introduction

CARBON fiber composites are highly suitable materials for aerospace applications due to their high strength to weight ratio.¹ However, the properties of these composites can only be selected from a linear spectrum ranging from full fiber to full matrix properties.² For next-generation applications, the usage of multiple reinforcements for the creation of hybrid carbon fiber composites is necessary in order to provide for a greater spectrum of selectable material properties. Carbon fiber composites have been explored with the inclusion of a variety of secondary reinforcements including: multiple fiber types,³ carbon nanotubes,⁴ and various other particulate inclusions.^{5,6} Alumina nanoparticles are particularly promising as a hybrid reinforcement

*Research Assistant, Mechanical and Aerospace Engineering, 12760 Pegasus Blvd, Orlando, FL 32816, and AIAA member

†Research Assistant, Department of Mechanical Engineering

‡ELEVATE Marie Curie Research Fellow, Department of Mechanical Engineering

§Reader in Materials Engineering, Department of Mechanical Engineering

¶Associate Professor, Mechanical and Aerospace Engineering (Joint appointments CREOL and MSE, Affiliated with CATER, NSTC), AIAA Associate Fellow, seetha.raghavan@ucf.edu

due to their improvement of mechanical properties such as elastic modulus and fracture toughness.⁷ Figure 1 shows a schematic for the potential application of these materials.

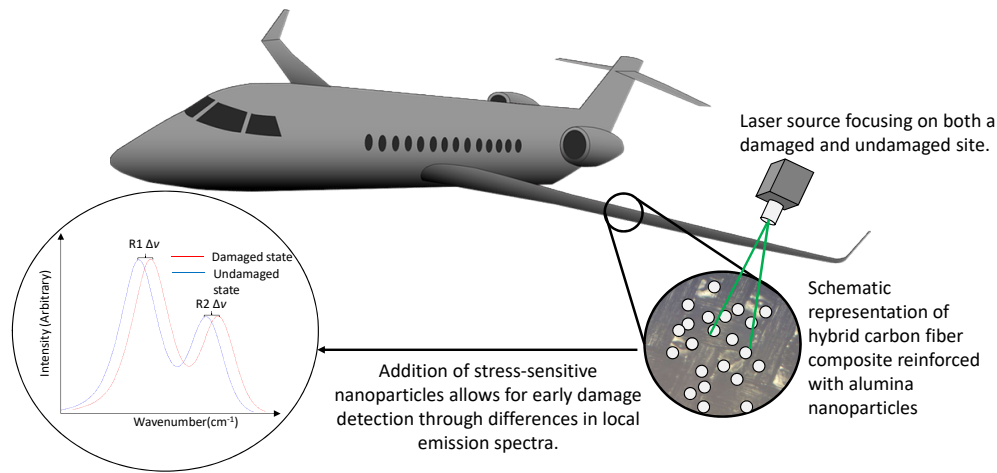


Figure 1. Schematic of an aerospace application of these hybrid carbon fiber composites due to improved mechanical properties and stress sensing capabilities.

These property improvements are highly dependent on the successful dispersion of the inclusions, as a homogeneous distribution of reinforcement provides better mechanical performance.⁸ Previous work developed photoluminescence spectroscopy as a novel method to measure particle dispersion in nanoparticle reinforced polymers.⁹ This technique was then applied to the investigation of the effects of particle loading on the dispersion of alumina nanoparticles in hybrid carbon fiber composites.^{10,11} This work found that increasing levels of particle loading resulted in an increased presence of particle agglomerates. These agglomerates can act as failure nucleation sites;¹² and, it is therefore imperative to assess methods for improving particle dispersion. This work explores the application of silane coupling agents as particle surface treatments. These coupling agents act as intermediary compounds which serve to reduce the net attractive force on each individual particle through a variety of mechanisms,^{13–16} ultimately improving dispersion. This is expected to allow for the maximum improvement to mechanical properties at higher weight percentages.^{8,17}

Furthermore, the photoluminescent emissions of alumina allows for the use of Piezoptroscopy.^{18–20} Piezospectroscopy is a technique for resolving stress from spectroscopic data and can be applied to the photoluminescent emissions of chromium (Cr^{3+}) doped alumina (Al_2O_3). These emissions from alumina, arise from the excitation of the chromium substitutional impurities which occupy sites with trigonal distortion.²¹ When these impurities are excited with a laser, the material emits photons over a wavelength spectra including the characteristic R-line doublets. It is known that the doublet emissions of chromium doped alumina shift linearly with applied stress and one form of this relationship is shown in Equation 1:¹⁹

$$\Delta v = \frac{1}{3} \Pi_{ii} \sigma_{ii} \quad (1)$$

where Δv is the wavenumber shift of the doublet emissions, Π_{ii} is the experimentally determined hydrostatic PS coefficient of alumina,²⁰ and $\frac{1}{3} \sigma_{ii}$ is the applied hydrostatic stress. These properties have been utilized in previous work for the development of stress-sensing epoxy nanocomposites.²² These nanocomposites have several applications, one of particular interest being their application as stress-sensing coatings that are capable of detecting the onset and propagation of sub-surface cracks in an underlying substrate.²³ Embedding these nanoparticles in carbon fiber composites enables the collection of internal particle stress measurements,^{10,24} which can reveal similar interlaminar cracking while simultaneously reinforcing the composite as a whole. Application of this measurement technique allows for simultaneous particle dispersion and stress characterization which can provide information on the effects of manufacturing parameters on the mechanical behavior of these composites. This allows for the manufacturing of next generation carbon fiber composites which have improved properties that can be selected based on particle and fiber volume fraction.

II. Experimental Methods

In order to utilize the stress sensing properties of the secondary alumina reinforcements, it is necessary to combine several different optical systems. These are combined into a Portable Piezospectroscopy System,²⁵ which uses a Princeton Instrument Pixis 100 charge coupled device, Acton SP2150 spectrometer, and an InPhotonics Inc. RPB Raman Probe. The laser used outputted approximately 14 mW from the end of the spectroscopic probe. This system is capable of measuring the local intensity of the photoluminescent (PL) response in addition to tracking the frequency of the emissions. In order to provide stress and intensity distributions across the sample surface, an XYZ stage is used in conjunction with the CCD to collect measurements in a snake scan pattern. While both peaks of the characteristic doublet are stress-sensitive, this work utilizes the R1 peak due to its higher intensity.²³ The samples manufactured were produced using a method known as resin infusion under flexible tooling (RIFT).²⁶ A schematic describing this method is shown in Figure 2.

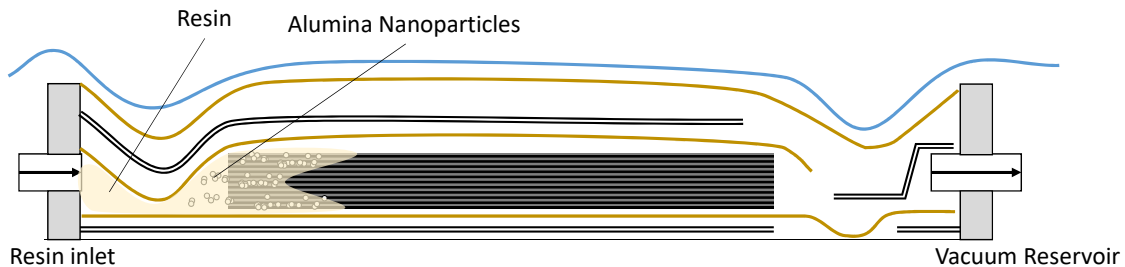


Figure 2. Schematic describing resin infusion under flexible tooling (RIFT) which utilizes a vacuum to drive the infusion of resin loaded with nanoparticles into a carbon fiber stack.

This technique allows for the infusion of nanoparticles while also providing for a void free composite. All tested samples were produced with a $57 \pm 3\%$ volume fraction of carbon fiber. The weight percentage of nanoparticles was adjusted, depending on the sample, to between 10 and 12 wt%. Each weight percentage was used to investigate different properties. The 10 wt% sample was used to determine any effects of particle dispersion on the stress distribution of these composites. It was tested using an MTS electromechanical load frame. Digital Image Correlation (DIC) was performed on the backside of the sample which provided verification for the piezospectroscopic stress results. Timing of data collection was important as interference was detected in the DIC measurements which resulted from the PS laser. To resolve this issue, DIC measurements were taken during load ramping and PS stress data was collected during force controlled holds every 1.05 kN. The equipment used is shown in Figure 3a and b and the loading profile is shown in Figure 3c. The scanning region was 10 mm x 50 mm and a resolution of approximately $300 \mu\text{m}$ was selected.

The primary difference between the 12 and 10 wt% samples, outside of particle loading, was the use of coupling agent surface treatments in the 12 wt% samples. The surface treatments investigated were a reactive and nonreactive silane coupling agent, gamma-glycidoxypolytrimethoxysilane and trimethoxysilyl respectively. The difference between these two is that the reactive coupling agent has organofunctional groups capable of bonding with the matrix while the non-reactive surface treatment only bonds to the particles. Both are expected to provide for improved particle dispersion, albeit through different mechanisms.⁸ The reactive treatment covalently bonds the particles to the matrix during the curing process preventing them from clustering.¹⁴ The non-reactive agent does not provide for the same bonding and simply reduces the surface energy of the particles, which decreases particle-particle interactions¹⁵ thereby minimizing the drive of the particles to cluster. A sample with untreated particles was also tested as a baseline for the interpretation of the effects of these surface treatments.

The photoluminescence of the treated samples was investigated using the same Portable Piezospectroscopy System.²⁵ These tests were conducted in a 10 mm x 40 mm scanning region with a spatial resolution of $200 \mu\text{m}$. Scans were conducted on the front and back faces of each sample in order to infer dispersion behavior of particles through sample thickness. All measurements presented are in the form of contour maps. In these maps, each pixel represents a specific characteristic of the R-lines at that point.

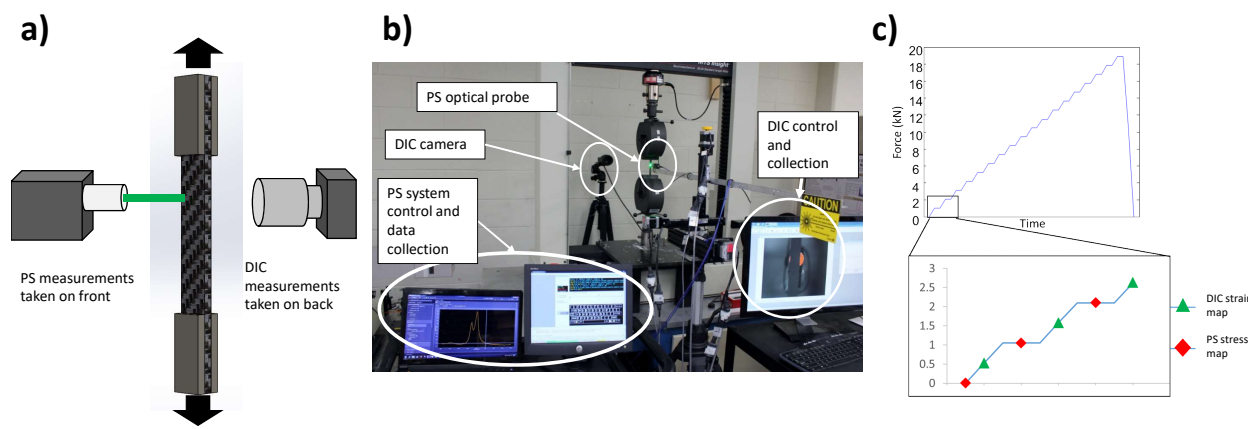


Figure 3. a) Schematic showing location of PS and DIC measurements on HCFRP sample b) Labeled experimental setup showcasing PS equipment setup, DIC equipment setup, and the mechanical load frame and c) Loading pattern applied to HCFRP samples showing the timing of DIC and PS measurements with the maximum achieved stress.

The peakshift of each spectra from the unloaded polycrystalline alumina peak position²⁷ can be calculated and then inputted into the PS relationship in order to resolve local stresses. While a direct conversion from intensity to particle concentration has not been established, relative concentration of particles across the sample surface can be investigated. Higher local intensities correlate to higher local particle concentrations, as an increased presence of chromium impurities in the scanning region results in more photon emissions which is measured as higher intensities. This allows for the comparison of the dispersion of samples with different surface treatments.

III. Results

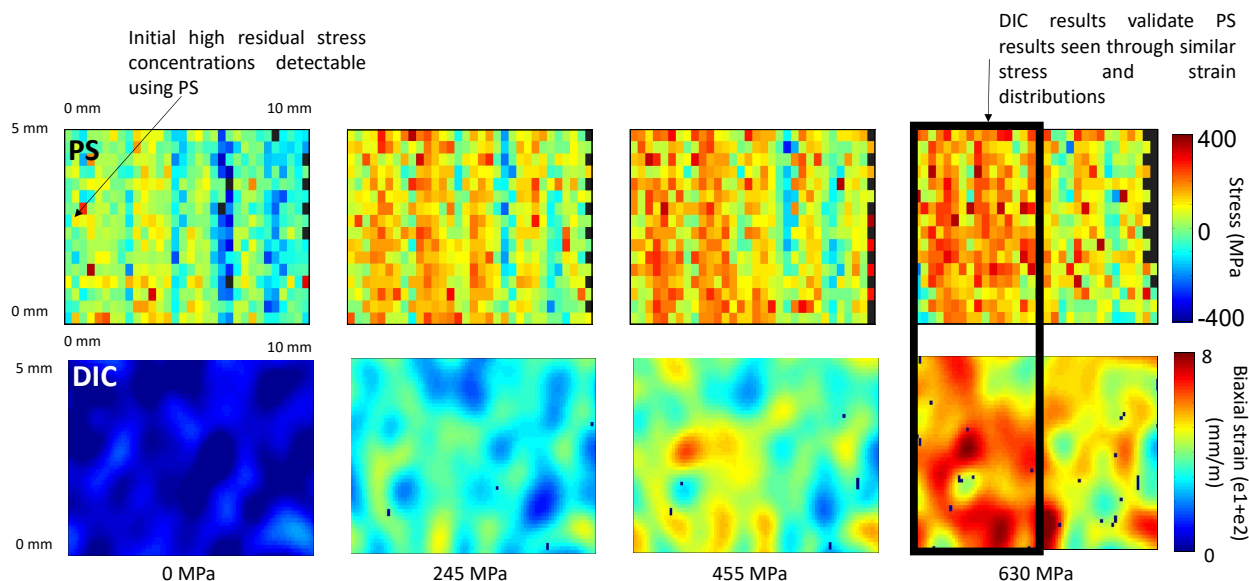


Figure 4. PS measurements on front face show internal stress distribution and backside DIC measurements show composite strains for mechanically loaded 10 wt% HCFRP specimen.

Stress and surface strain maps are compared in Figure 4. There is a resolution mismatch with the PS measurements having a spatial resolution of approximately $300 \mu\text{m}$ and the DIC measurements having a

higher resolution of approximately $90\ \mu\text{m}$. This lower PS resolution arose from a necessary optimization of collection parameters for short times during the force controlled holds. Internal stress concentrations are measured by PS and were observed to be aligned in a columnar manner. While similar stress distributions were not detected with DIC, both measurements agree that the left region of the sample is the likely failure zone. The differences in distribution shape of these techniques arise from the different parts of the sample being investigated. The DIC measurements report surface composite strain, and so provide deformations that result on the surface of the sample. The PS technique is unique in that in this sample configuration, the stress values reported are from the alumina nanoparticles. As such, the stress measurements are indicative of matrix to particle load transfer, and the columnar stress distributions noted indicate inhomogeneity in matrix properties across the scanning surface.

These columnar stress concentrations are seen to arise from particle agglomerations which can be detected through the PL intensity distributions. The distribution of intensities in the photoluminescence profile match very closely to the stress profile presented in Figure 5, which shows the stress profile for the investigated region with different loads and the accompanying intensity distribution at zero load. There is a clear match between the areas of high intensity and high stress; and, since it is established that the local intensity of the emissions provides for local particle concentrations, it is found in this work that the areas with high particle concentrations exhibit higher stress upon mechanical loading of the samples.

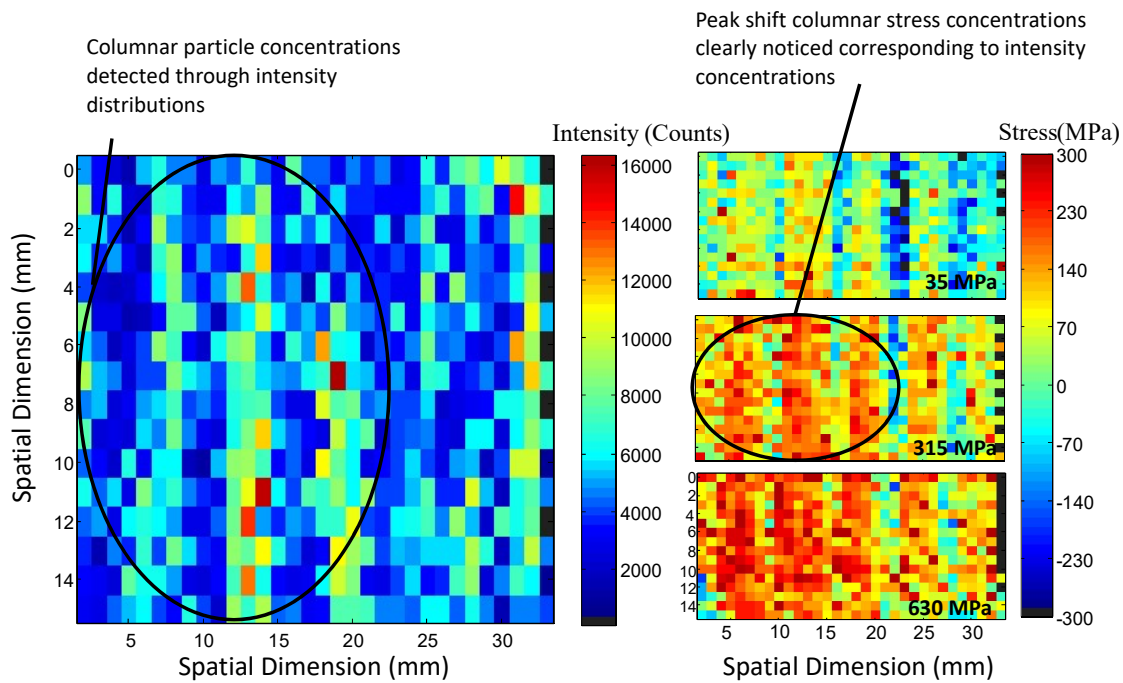


Figure 5. Comparison of intensity profile to stress profile shows the resulting match of particle agglomerations to stress concentrations at various loading stresses.

In order to further investigate the properties of these composites, a small homogeneous region is selected for the comparison of local stress from PS measurements and strains from DIC measurements. These values are then plotted in order to view nanoparticle behavior versus overall composite behavior. Figure 6 shows a somewhat linear trend initially between particle peak shift and composite strain. At higher composite strains this behavior begins to breakdown and a maximum peak shift is reached. This behavior is indicative of interfacial failure between the particles and matrix resulting in reduced load transfer¹⁰ which indicates failure initiation.

The findings regarding particle clusters acting as stress concentrators and a poor particle-matrix interface necessitates the investigation of the previously described coupling agents. Their application is expected to improve dispersion, and in the case of the reactive treatment specifically also improve the strength of the

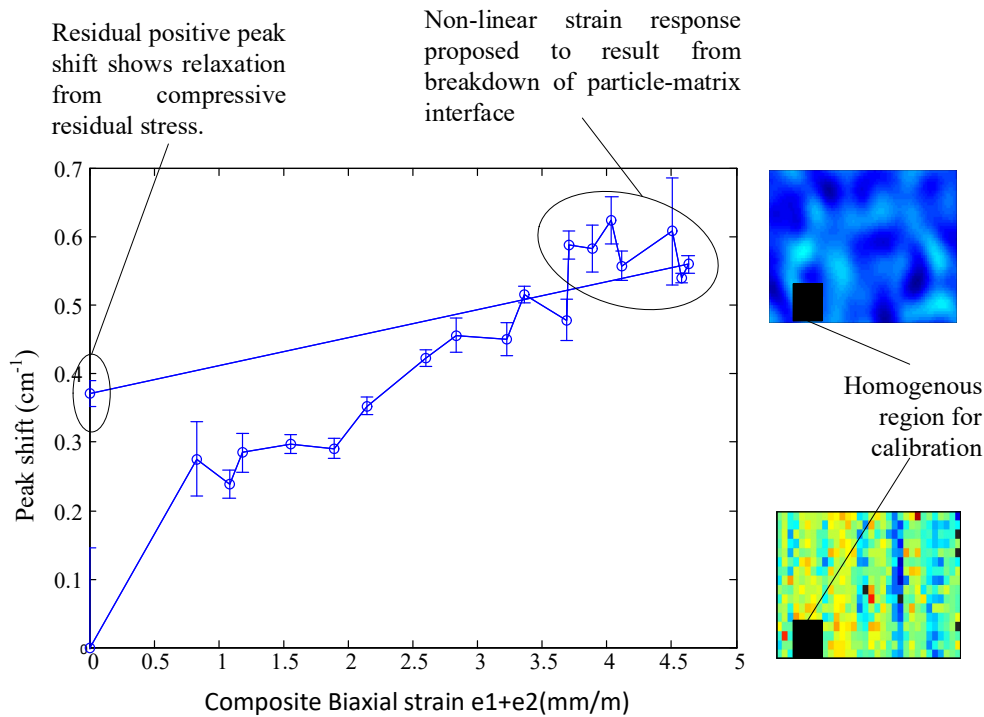


Figure 6. Particle stress vs composite biaxial strain shows particle behavior with increasing composite loading.

particle-matrix interface. In the current work, the effects of the coupling agents on particle dispersion is presented for untreated, RSCA treated and NRSCA treated samples. Contour maps for 12 wt% samples with and without treatments are shown in Figure 7.

For the analysis of these contour maps it is necessary to consider two primary factors related to overall sample dispersion. The first factor is the distribution of particles. In an ideally dispersed sample all pixels have the same intensity which correlates to equal particle concentrations across the surface. Alternatively, samples dominated by high intensity gradients have poor dispersion. This is characterized by the presence of regions which have high intensities surrounded by regions with very low intensities. Furthermore, another factor necessary for understanding particle dispersion is the sedimentation of particles. This is characterized by an intensity mismatch between the front and back faces, and is indicative of poor particle dispersion through sample thickness. Both factors must be taken into account when comparing sample dispersion.

For the presented contour maps, the first analysis done will be with respect to particle distributions. The sample dominated most by large intensity gradients is the untreated 12 wt% side B sample. The presence of these large intensity gradients is mitigated with the application of the surface treatments. The higher intensity side of the RSCA and NRSCA treated samples, side B and side A respectively, both have more homogeneous intensities throughout the sample surface than the untreated sample. The RSCA treated sample is seen to have better dispersion than the NRSCA treated sample, which indicates that at these high weight percentages the reduction in surface energy provided by the NRSCA treatment is not sufficient to counteract the increased particle attractive forces. With respect to sedimentation, the treatments again are seen to provide improvements. The untreated side A and side B have large intensity mismatches, with a majority of intensity present on Side B. This indicates that the particles are primarily concentrated on side B and that there is likely a significant dispersion gradient through thickness. This intensity mismatch is reduced with the NRSCA treatment and almost non-existent in the RSCA treated sample. It is confirmed again that at this high weight percentage, the RSCA surface treatment provides for the largest benefits to particle dispersion.

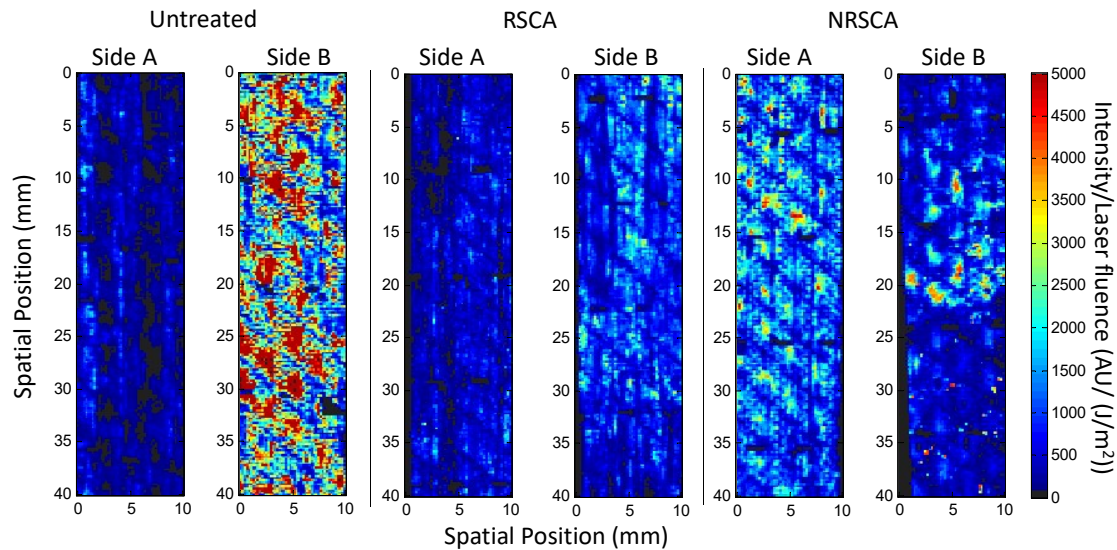


Figure 7. Dispersion contour maps for both sides of each 12 wt% sample shows dispersion improvement with application of particle surface treatment.

IV. Conclusion

Carbon fiber composites were designed and manufactured with the addition of secondary alumina nanoparticle reinforcements. Utilizing piezospectroscopy, the difference in particle stress within different matrix regions can be quantified through the tracking of the energy of their PL emissions. These investigations found that with applied loads, stress concentrations tended to form in regions with higher PL intensities. This shows the importance of a well dispersed reinforcement, as higher local particle concentrations are associated with higher local stresses. Further investigation, through the comparison of DIC strain and PS peak shift, found interfacial failure between the particles and matrix at higher loads. In order to address these issues, silane coupling agents are explored. Application of silane coupling agents as particle surface treatments is found to improve dispersion of particles in HCFRPs. The reactive coupling agent was found to be more effective at higher weight percentages, likely due to the covalent bonding mechanism. Future mechanical tests will show the improvements to mechanical properties associated with the improved dispersion and improved particle/matrix interface from the applied particle surface treatments.

Acknowledgements

This work was supported by University of Central Florida's International Affairs and Global Strategies In-house grant and the NSF Innovation through Institutionalized Integration (ICubed) Fellowship.

References

- ¹Soutis, C., "Carbon fiber reinforced plastics in aircraft construction," *Materials Science and Engineering A*, Vol. 412, No. 1, 2005, pp. 171–176.
- ²Xu, Y. and Hoa, S. V., "Mechanical properties of carbon fiber reinforced epoxy/clay nanocomposites," *Composites Science and Technology*, Vol. 68, 2008, pp. 854–861.
- ³Dutra, R., Soares, B., Campos, E., and Silva, J., "Hybrid composites based on polypropylene and carbon fiber and epoxy matrix," *Polymer*, Vol. 41, No. 10, 2000, pp. 3841–3849.
- ⁴Zhang, F. H., Wang, R. G., He, X. D., Wang, C., and Ren, L. N., "Interfacial shearing strength and reinforcing mechanisms of an epoxy composite reinforced using a carbon nanotube/carbon fiber hybrid," *Journal of Materials Science*, Vol. 44, No. 13, 2009, pp. 3574–3577.
- ⁵Cho, J., Chen, J. Y., and Daniel, I. M., "Mechanical enhancement of carbon fiber/epoxy composites by graphite nanoplatelet reinforcement," *Scripta Materialia*, Vol. 56, No. 8, 2007, pp. 685–688.
- ⁶Timmerman, J. F., Hayes, B. S., and Seferis, J. C., "Nanoclay reinforcement effects on the cryogenic microcracking of carbon fiber/epoxy composites," *Composites Science and Technology*, Vol. 62, 2002, pp. 1249–1258.

- ⁷Hussain, M., Nakahira, A., and Niihara, K., "Mechanical property improvement of carbon fiber reinforced epoxy composites by Al₂O₃ filler dispersion," *Materials Letters*, Vol. 26, No. 3, 1996, pp. 185–191.
- ⁸Vassileva, E. and Friedrich, K., "Epoxy/alumina nanoparticle composites. II. Influence of silane coupling agent treatment on mechanical performance and wear resistance," *Journal of Applied Polymer Science*, Vol. 101, No. 6, 2006, pp. 4410–4417.
- ⁹Stevenson, A. L., *Calibration of Alumina-Epoxy Nanocomposites Using Piezospectroscopy for the Development of Stress-Sensing Adhesives*, Masters thesis, University of Central Florida, 2011.
- ¹⁰Hanhan, I., *Hybrid Carbon Fiber Alumina Nanocomposite for Non-Contact Stress Sensing via Piezospectroscopy*, Honors in the Major thesis, University of Central Florida, 2015.
- ¹¹Hanhan, I., Selimov, A., Raghavan, S., Carolan, D., and Taylor, A. C., "Quantifying alumina nanoparticle dispersion in hybrid carbon fiber composites using photo-luminescent spectroscopy," *Applied Spectroscopy*, 2016, In Press.
- ¹²Schmauder, S., Weber, U., and Soppa, E., "Computational mechanics of heterogeneous materials influence of residual stresses," *Computational Materials Science*, Vol. 26, 2003, pp. 142–153.
- ¹³Plueddemann, E. P., *Silane Coupling Agents*, Plenum Press, New York; London, 2nd ed., 1991.
- ¹⁴Shokoohi, S., Arefazar, A., and Khosrokhavar, R., "Silane Coupling Agents in Polymer-based Reinforced Composites: A Review," *Journal of Reinforced Plastics and Composites*, Vol. 27, No. 5, 2008, pp. 473–485.
- ¹⁵Demjén, Z., Pukánszky, B., and Nagy, J., "Evaluation of interfacial interaction in polypropylene/surface treated CaCO₃ composites," *Composites Part A: Applied Science and Manufacturing*, Vol. 29, No. 3, 1998, pp. 323–329.
- ¹⁶Condon, J. R. and Ferracane, J. L., "Reduced polymerization stress through non-bonded nanofiller particles," *Biomaterials*, Vol. 23, No. 18, 2002, pp. 3807–3815.
- ¹⁷Shahid, N., Villate, R. G., and Barron, A. R., "Chemically functionalized alumina nanoparticle effect on carbon fiber/epoxy composites," *Composites Science and Technology*, Vol. 65, No. 14, 2005, pp. 2250–2258.
- ¹⁸Grabner, L., "Spectroscopic technique for the measurement of residual stress in sintered Al₂O₃," *Journal of Applied Physics*, Vol. 49, No. 2, 1978, pp. 580–583.
- ¹⁹Ma, Q. and Clarke, D. R., "Stress Measurement in Single-Crystal and Polycrystalline Ceramics using their Optical Fluorescence," *Journal of the American Ceramic Society*, Vol. 76, No. 6, 1993, pp. 1433–1440.
- ²⁰He, J. and Clarke, D. R., "Determination of the Piezospectroscopic Coefficients for Chromium-Doped Sapphire," *J. Am. Ceram. Soc.*, Vol. 78, No. 5, 1995, pp. 1347–1353.
- ²¹Hough, H., Demas, J., Williams, T. O., and Wadley, H. N. G., "Luminescence Sensing of Stress in Ti/Al₂O₃ Fiber Reinforced Composites," *Acta Metallurgica et Materialia*, Vol. 43, No. 2, 1995, pp. 821–834.
- ²²Stevenson, A., Jones, A., and Raghavan, S., "Stress-Sensing Nanomaterial Calibrated with Photostimulated Luminescence Emission," *Nano Letters*, Vol. 11, No. 8, 2011, pp. 3274–3278.
- ²³Freihofer, G. J., *Nanocomposite Coating Mechanics via Piezospectroscopy*, Doctoral dissertation, University of Central Florida, 2014.
- ²⁴Hanhan, I., Selimov, A., Carolan, D., Taylor, A., and Raghavan, S., "Characterizing Mechanical Properties of Hybrid Alumina Carbon Fiber Composites with Piezospectroscopy," *57th AIAA/ASCE/AHS/ASC Structures, Structural Dynamics, and Materials Conference*, 2016, p. 1413.
- ²⁵Hanhan, I., Durnberg, E., Freihofer, G., Akin, P., and Raghavan, S., "Portable Piezospectroscopy system: non-contact in-situ stress sensing through high resolution photo-luminescent mapping," *Journal of Instrumentation*, Vol. 9, No. 11, 2014, pp. P11005.
- ²⁶Hsieh, T. H., Kinloch, A. J., Masania, K., Sohn Lee, J., Taylor, A. C., and Sprenger, S., "The toughness of epoxy polymers and fibre composites modified with rubber microparticles and silica nanoparticles," *Journal of Materials Science*, Vol. 45, No. 5, 2010, pp. 1193–1210.
- ²⁷He, J., Beyerlein, I. J., and Clarke, D. R., "Load transfer from broken fibers in continuous fiber Al₂O₃-Al composites and dependence on local volume fraction," *Journal of the Mechanics and Physics of Solids*, Vol. 47, No. 3, 1999, pp. 465–502.